BRIEF REPORT

ENVIRONMENTAL MICROBIOLOGY | Applied Microbiology International

Acetic acid stress response of the acidophilic sulfate reducer *Acididesulfobacillus acetoxydans*

Reinier A. Egas[1] [ORCID] | Diana X. Sahonero-Canavesi[2] | Nicole J. Bale[2] | Michel Koenen[2] | Çağlar Yildiz[1] | Laura Villanueva[2,3] | Diana Z. Sousa[1,4] | Irene Sánchez-Andrea[1,5]

[1]Laboratory of Microbiology, Wageningen University & Research, Wageningen, The Netherlands

[2]Department of Marine Microbiology and Biogeochemistry, Royal Netherlands Institute for Sea Research (NIOZ), Texel, Den Burg, The Netherlands

[3]Department of Earth Sciences, Utrecht University, Utrecht, The Netherlands

[4]Centre for Living Technologies, Alliance TU/e, WUR, UU, UMC Utrecht, Utrecht, The Netherlands

[5]Environmental Sciences and Sustainability Department, Science & Technology School, IE University, Segovia, Spain

Correspondence
Irene Sánchez-Andrea, Laboratory of Microbiology, Wageningen University & Research, Stippeneng 4, Wageningen 6708, The Netherlands.
Email: irene.sanchezandrea@wur.nl

Funding information
Soehngen Institute for Anaerobic Microbiology Gravitation Program, Grant/Award Number: SIAM 024.002.002; Gravitation Grant of the Netherlands Ministry of Education, Culture and Science

Abstract

Acid mine drainage (AMD) waters are a severe environmental threat, due to their high metal content and low pH (pH <3). Current technologies treating AMD utilize neutrophilic sulfate-reducing microorganisms (SRMs), but acidophilic SRM could offer advantages. As AMDs are low in organics these processes require electron donor addition, which is often incompletely oxidized into organic acids (e.g., acetic acid). At low pH, acetic acid is undissociated and toxic to microorganisms. We investigated the stress response of the acetotrophic *Acididesulfobacillus acetoxydans* to acetic acid. *A. acetoxydans* was cultivated in bioreactors at pH 5.0 (optimum). For stress experiments, triplicate reactors were spiked until 7.5 mM of acetic acid and compared with (non-spiked) triplicate reactors for physiological, transcriptomic, and membrane lipid changes. After acetic acid spiking, the optical density initially dropped, followed by an adaptation phase during which growth resumed at a lower growth rate. Transcriptome analysis revealed a downregulation of genes involved in glutamate and aspartate synthesis following spiking. Membrane lipid analysis revealed a decrease in *iso* and *anteiso* fatty acid relative abundance; and an increase of acetyl-CoA as a fatty acid precursor. These adaptations allow *A. acetoxydans* to detoxify acetic acid, creating milder conditions for other microorganisms in AMD environments.

INTRODUCTION

Acid rock and acid mine drainages (ARD and AMD) are streams characterized by their low pH (<3), and high concentrations of sulfate, and heavy metals (Hedrich & Schippers, 2020; Johnson & Hallberg, 2005; Parbhakar-Fox & Lottermoser, 2015). If not mitigated, AMD and ARD can have a detrimental impact on water quality and biodiversity (Hallberg, 2010; Kefeni et al., 2017; Park et al., 2019).

Bioremediation is an active biological process that can be used to treat ARD and AMD focusing on the removal of heavy metals and increase in water pH (Johnson & Sánchez-Andrea, 2019; Ňancucheo et al., 2017). Of particular interest for bioremediation are sulfate-reducing microorganisms (SRM), which through dissimilatory sulfate reduction can convert sulfate to sulfide. Produced sulfide then reacts with metals to form highly insoluble metal sulfides, effectively removing them from the liquid fraction (Johnson & Santos, 2020; Peiffer, 2016; van der Graaf et al., 2020). The solubility of different metal sulfides is pH dependent, enabling their selective precipitation through pH control (Ňancucheo & Johnson, 2012; Santos &

Johnson, 2018). In addition, SRM can increase the pH as, at low pH, the reduction of sulfate to sulfide consumes protons (Johnson & Sánchez-Andrea, 2019). To date, industrial-scale biosulfidogenic processes are using neutrophilic microorganisms requiring pH neutralization of the influent (Johnson & Santos, 2020; Ñancucheo & Barrie Johnson, 2014). Utilization of acidophilic SRM (aSRM) could be economically beneficial, as it would avoid the pH neutralization step (Johnson & Sánchez-Andrea, 2019; Sánchez-Andrea et al., 2014).

In sulfidogenic processes often an electron donor, for example, lactate or glycerol, is supplemented to increase sulfate reduction rates, as AMD and ARD generally contain low concentrations of organic carbon (Sánchez-España et al., 2020). Acetic acid is a common intermediate in the oxidation of these substrates, which accumulates in the reactors. From a processing perspective, acetic acid accumulation is an economical loss as it can be considered unused substrate and electron donor (Kaksonen et al., 2004; Santos & Johnson, 2018, 2022). Additionally, from a biological perspective, acetic acid (pK_a of 4.76) can be toxic to microorganisms at low pH, since the proportion of the undissociated (acid) form of acetic acid increases in acidic conditions. The undissociated form of acetic acid can freely diffuse into the cell (Alexander et al., 1987; Grime et al., 2008). Inside the cell, due to the higher cytoplasmic pH, acetic acid dissociates releasing a proton and the acetate anion (Herrero et al., 1985; Slonczewski et al., 2009). Released protons acidify the cytoplasm, requiring energy expenditure for pH homeostasis with mechanisms such as proton pumps and amino acid decarboxylation (Baker-Austin & Dopson, 2007; Boase et al., 2022; Trček et al., 2015). Anion accumulation affects the internal anion pool and membrane potential, hampering metabolic activity and growth (Alexander et al., 1987; Pinhal et al., 2019; Roe et al., 1998). To prevent acetic acid from diffusing into the cell, adjusting membrane permeability has been suggested to play a crucial role (Lindberg et al., 2013; Xia & Yuan, 2009).

Complete oxidation of organic acids, such as acetic acid, to CO_2 would alleviate stress on aSRM. Next to this, the ability to completely oxidize organic acids holds other advantages. First, complete oxidation gives aSRM the environmental advantage of being able to use the often available electron donor, second it consumes more protons compared to incomplete oxidation neutralizing the acidic pH. Nevertheless, the complete oxidation of organic acids is an uncommon metabolic trait of aSRM. Of the seven fully described and isolated acidophilic sulfate reducing bacteria (aSRB), only *Acididesulfobacillus acetoxydans* can completely oxidize acetic acid to CO_2 through the oxidative acetyl-CoA pathway (Alazard et al., 2010; Frolov et al., 2017; Mori et al., 2003; Panova et al., 2021; Sánchez-Andrea et al., 2013, 2015, 2022). Thus, *A. acetoxydans* is an

excellent model microorganism to study acetic acid stress-relief strategies of aSRB.

With *A. acetoxydans* as model organism this study aims to identify the mechanisms employed by aSRB to handle acetic acid toxicity. We hypothesized that acetic acid toxicity would, aside from acetic acid oxidation, result in an increased expression of proton and anion homeostasis mechanisms. Likely this is combined with membrane adaptations to prevent entry of acetic acid. To test these hypotheses two main experimental steps were performed. First, the sub-lethal concentration of acetic acid was determined through spiking mid-exponential phase *A. acetoxydans* cultures with different concentrations of acetic acid in pH-controlled bioreactors. Second, cultures grown at the maximum identified tolerated acetic acid concentration were compared to cultures grown in non-stressed control reactors. We followed a multifaceted approach by comparing both conditions through physiological, gene expression and membrane lipid analyses.

EXPERIMENTAL PROCEDURES

Microorganism and cultivation medium

Acididesulfobacillus acetoxydans DSM 29876[T] was retrieved from our culture collection at the Laboratory of Microbiology (Wageningen University & Research). Unless otherwise specified chemicals were obtained from Sigma-Aldrich (Merck KGaA, Darmstadt, Germany). Basal medium was prepared as described previously (Stams et al., 1993). The bicarbonate buffer was omitted to allow pH adjustment of the media to pH 5 by using HCl and NaOH. Serum bottles (217 mL) were filled with 100 mL of basal medium, closed with rubber stoppers and aluminium cramps, and the headspace flushed and filled with N_2/CO_2 (1.5 atm, 80/20 v/v). Before inoculating with *A. acetoxydans* (inoculum 1% v/v), medium was reduced with 1.5 mM of L-cysteine and supplemented with trace elements and vitamins (Stams et al., 1993), 5 mM glycerol, 0.1 g L^{-1} yeast extract and 20 mM sodium sulfate. All supplement additions were done from autoclaved anoxic stock solutions, except the vitamins' solution, which was filter-sterilized through a 0.22 μm pore-size polyethersulfone filter (Advanced Microdevices, Tepla, India). Serum bottles were incubated statically at 30°C.

Acetic acid stress tests

Acetic acid stress experiments were performed in triplicate using bioreactors with a working volume of 1 L in 1.3 L DASGIP Parallel Bioreactors (Eppendorf, Hamburg, Germany). Reactors were also equipped with a redox probe (Hamilton, Reno, NV, USA). The whole reactor system, including basal medium, was

TABLE 1 Overview of reactors run in this study, for each experiment all bioreactors were run simultaneously. For each condition in the stress comparison experiment, the sampling times for either transcriptomics or core lipid analysis are indicated relative to the moment after spiking.

Exp 1. Acetic acid toxicity		Exp 2. Stress response mechanisms			
Bioreactors	Acetic acid spike (mM)	Bioreactors	Acetic acid spike (mM)	Sampling time transcriptome	Sampling time core lipid analysis
1 (control)	0	1–3 (control)	0	2.5 h	—
2, 3	5	4–6 (stressed)	7.5	2.5 h, 26 h	8 days
4, 5	7.5	7, 8 (control)	0	—	2.5 h
6, 7	10				

autoclaved to allow sterile operation. After autoclavation, reactors were flushed overnight with N_2 and subsequently reducing agent, trace elements, vitamins and glycerol were added from sterile stock solutions as described above. Temperature was maintained at 30°C, an agitation rate of 100 rpm was used and the pH was controlled at 5.0 by addition of 0.5 M HCl. To maintain anoxic conditions, and to prevent sulfide accumulation, the reactors were continuously sparged with N_2/CO_2 (80/20 v/v) at a rate of 5 L h^{-1}. A mid-exponential phase culture of *A. acetoxydans* was used to inoculate each reactor (inoculum 1% v/v). Growth was monitored off-line by measuring optical density at 600 nm (OD_{600}) using a Shimadzu UV-1800 spectrophotometer (Shimadzu, Kyoto, Japan).

For the acetic acid toxicity test (experiment 1), cells of *A. acetoxydans* were inoculated in 7 reactors containing anoxic basal medium supplemented with 5 mM glycerol and 20 mM sodium sulfate. When cultures reached 70% of maximum OD_{600}, reactors were spiked with acetic acid to final concentrations of 5.0, 7.5 or 10.0 mM (duplicates per condition, Table 1). Additionally, there was a control reactor, which was operated without acetic acid spiking. For the acetic acid stress response mechanisms (experiment 2), reactors were spiked with 7.5 mM acetic acid (final concentration). Both control and acetic acid spiked cultivations were performed in triplicate. Samples for transcriptome analyses were taken at two time points after spiking, that is, 2.5 and 26 h after spiking. The first time-point sample was withdrawn from both spiked and control reactors. At day 5 post-spiking, additional 5 mM of sulfate was added to the test reactors; and at day 6, again 5 mM sulfate and 5.5 mM acetic acid. At day 8 post-spiking, samples were taken for lipid analyses (spiked condition). For lipid analysis, two extra control reactors were operated to prevent interference of sampling on the transcriptome of the control tests. Of these reactors lipid samples were taken at 70% of the maximum OD_{600} to function as control.

Extracellular metabolite analysis

Glycerol and acetate were measured by high-performance liquid chromatography (HPLC) on a Shimadzu LC2030c plus (Shimadzu, Kyoto, Japan) equipped with a Shodex SH1821 column (Shodex, Tokyo, Japan) and a Shimadzu RID-20A differential refractive index detector (Shimadzu, Kyoto, Japan). A solution of 5 mM sulfuric acid was used as eluent at a flow of 0.8 mL min^{-1}, and the column was kept at 45°C. Arabinose (10 mM) was used as internal standard. For each timepoint, the acetic acid concentrations were corrected through the Henderson-Hasselbalch equation for the pH effect, hence acetic acid concentrations depict solely the protonated form. ʟ-cysteine was measured by HPLC, after a derivatization pre-treatment with 1.3 mg mL^{-1} dabsyl chloride dissolved in acetonitrile (Vendrell & Avilés, 1986). Supernatant of the derivatization mixture was analysed on the aforementioned Shimadzu LC2030c plus, but equipped with a Poroshell 120EC-C18 column (Agilent, Santa Clara, CA, USA). Sulfate was measured using anion exchange chromatography on a Dionex ICS-2100 (Dionex, Sunnyvale, CA, USA) equipped with a Dionex IonPac AS16 column (Dionex, Sunnyvale, CA, USA) operated at 30°C. As eluent potassium hydroxide (22%) was used in a gradient ranging from 10 to 40 mM and with a flow rate of 0.4 mL min^{-1}. For all measured compounds, the detection limit was approximately 100 μM.

Transcriptomics

150 mL of culture was taken from each reactor and immediately added to 100 mL of ice cold sterile reduced medium. The cell suspension was centrifuged at 10,000 × g for 10 min at 4°C (ThermoFisher, Waltham, MA, USA). Then, the pellet was resuspended in 10 mL TE buffer (10 mM tris–HCl, 0.1 mM EDTA, pH 8), transferred to 50 mL sterile tubes (Greiner, Frickenhausen, Germany) and centrifuged again. Obtained pellet was snap-frozen in liquid nitrogen and stored at −80°C until further processing. The MasterPure Gram Positive DNA Purification kit (Epicentre, Madison, WI, USA) was used to lyse the cells and precipitate the proteins, skipping the RNase A step. β-mercaptoethanol was added to the lysis solution to inactivate present RNases. RNA was isolated from the obtained supernatant using the Maxwell® 16 LEV simplyRNA Purification

kit on the Maxwell® 16 platform (Promega, Madison, USA). RNA quality and quantity were assessed using the ratio of absorbances at 230, 260 and 280 nm (A_{260}/A_{230}, A_{260}/A_{280}) in a Nanodrop (DeNovix, Wilmington, DE, USA), a capillary gel electrophoresis system (BiOptic, New Taipei City, Taiwan) and a Qubit fluorometer (DeNovix, Wilmington, DE, USA). Purified RNA samples were stored at −80°C. Samples were sent to Novogene (Novogene, Cambridge, UK) for sequencing analysis. Ribosomal RNA was removed with the Ribo-Zero Plus rRNA depletion kit prior sequencing using the NovaSeq6000 (Illumina, San Diego, CA, USA) resulting in paired-end reads of 150 bp.

Raw sequence data were trimmed for Illumina adapters and paired using *Trimmomatic* 0.38 (Bolger et al., 2014) with the following settings: SLIDINGWINDOW: 4 bases, quality ≥20, average read score >5, MINLEN: 100, LEADING: 3, TRAILING: 3. Quality trimmed paired-end reads were checked using *FastQC* 0.11.9 and *MultiQC* 1.11 (Andrews et al., 2015; Ewels et al., 2016). The reads were mapped against the reference genome of *A. acetoxydans* (GenBank accession number LR746496) (using *BWA-MEM* 0.7.17.2, Li & Durbin, 2010). Before mapping, 66 structural RNA (rRNA, sRNA and tRNA) genes were removed from the dataset. Count matrices with mapped reads were obtained using *featureCounts* 2.0.1 with paired-end reads enabled (Liao et al., 2014). Mapping quality was assessed with *SAMtools* (flagstat) 2.0.4. showing an average of 86% correctly mapped reads (Li et al., 2009). Mapped reads were converted to transcripts per million (TPM) to compare expression levels within samples. Genes are considered expressed with a TPM ≥10. Low, medium and high expression levels were assigned to genes with 10–50, 50–300 and >300 TPM. To test for significant statistical differences in gene expression between groups, the read counts were analysed with the R package *DESeq2* 1.30.1 (Love et al., 2014) using R 4.2.1. Differentially expressed genes were identified as genes with an expression change of at least fourfold and an adjusted p < 0.01. Functional categories were used for general analysis and were defined by assigning *A. acetoxydans* genes to clusters of orthologous groups (COGs) using eggNOG 5.0 (Huerta-Cepas et al., 2019).

Lipid analysis

This study analysed the core lipids, which are derived after hydrolysis as these comprise the glycerol backbone of the more complex membrane lipids. These include fatty acid methyl esters (FAMEs, derived from hydrolysis of the intact polar lipids), hydroxy FAMEs, dimethylacetals (DMAs; formed upon acid hydrolysis of plasmalogens) and mono alkyl glycerols (derived from non-plasmalogen ether lipids, also known as alkyl

ethers). For core lipid analysis, 350 mL of culture was taken, following the same procedure previously described for transcriptome sampling. The obtained pellets were resuspended in phosphate buffered saline solution (0.01 M phosphate, 0.27 mM KCl, 0.137 M NaCl pH 7.4), stored overnight at −20°C, and finally lyophilized and stored at 4°C. Extraction and analysis was performed as described previously (Bale et al., 2019). Briefly, aliquots of the lyophilized pellets were hydrolysed by refluxing in a 1.5 N HCl and MeOH solution for 3 h. After adjustment to pH 4–5 with a 2 N KOH/MeOH (1/1, v/v) solution, extraction with dichloromethane was performed. The resulting extract was methylated with diazomethane in diethyl ether and hydroxy groups were derivatized with N,O-Bis(trimethylsilyl)trifluoroacetamide (BSTFA) in pyridine. Compound identification was carried out using gas chromatography–mass spectrometry (Thermo Finnigan, San Francisco, CA, USA). Compounds were identified based on literature data and library mass spectra. Double bond positions were determined, where possible, using dimethyldisulfide (DMDS) derivatization.

RESULTS AND DISCUSSION

Acetic acid spike lowers growth rates of *A. acetoxydans*

We aimed to reveal how acetic acid impacts the metabolism of *A. acetoxydans* and to identify the maximum tolerated sub-lethal acetic acid spiking concentration of *A. acetoxydans*. For that, exponentially growing cells of *A. acetoxydans* at an OD_{600} of approximately 0.35 (corresponding to 70% of the maximum OD_{600} in these conditions) were spiked with acetic acid until a 5.0, 7.5, or 10.0 mM final concentration of acetic acid (protonated, toxic form).

After spiking, the OD_{600} dropped in all the cultures, this effect being more pronounced with increasing acetic acid concentrations (Figure 1A). After an adaptation phase, cultures spiked with 5.0 and 7.5 mM acetic acid resumed growth, but not the cultures spiked it 10.0 mM. Growth rates were also affected, prior spiking, the doubling times for all cultures were on average (mean ± standard deviation) 17.1 ± 0.2 h^{-1}. However, after spiking, the doubling time increased to 239.4 h^{-1} and 546.5 h^{-1} for the 5.0 and 7.5 mM spiked cultures, respectively. As no sulphur intermediates, such as sulfite, were detected, the amount of electrons donated per increase of 0.1 OD_{600} can be calculated (8 electrons per sulfate) to gauge energy expenditure. Prior spiking, approximately 1.15 mM sulfate was reduced (equivalent to 9.22 mM e$^-$ donated) for an increase of 0.1 OD_{600}. Afterwards, this number increased to 4.65 and 7.47 mM sulfate (37.2 and 59.7 mM e$^-$), for spiking until 5.0 and 7.5 mM acetic acid, respectively. This
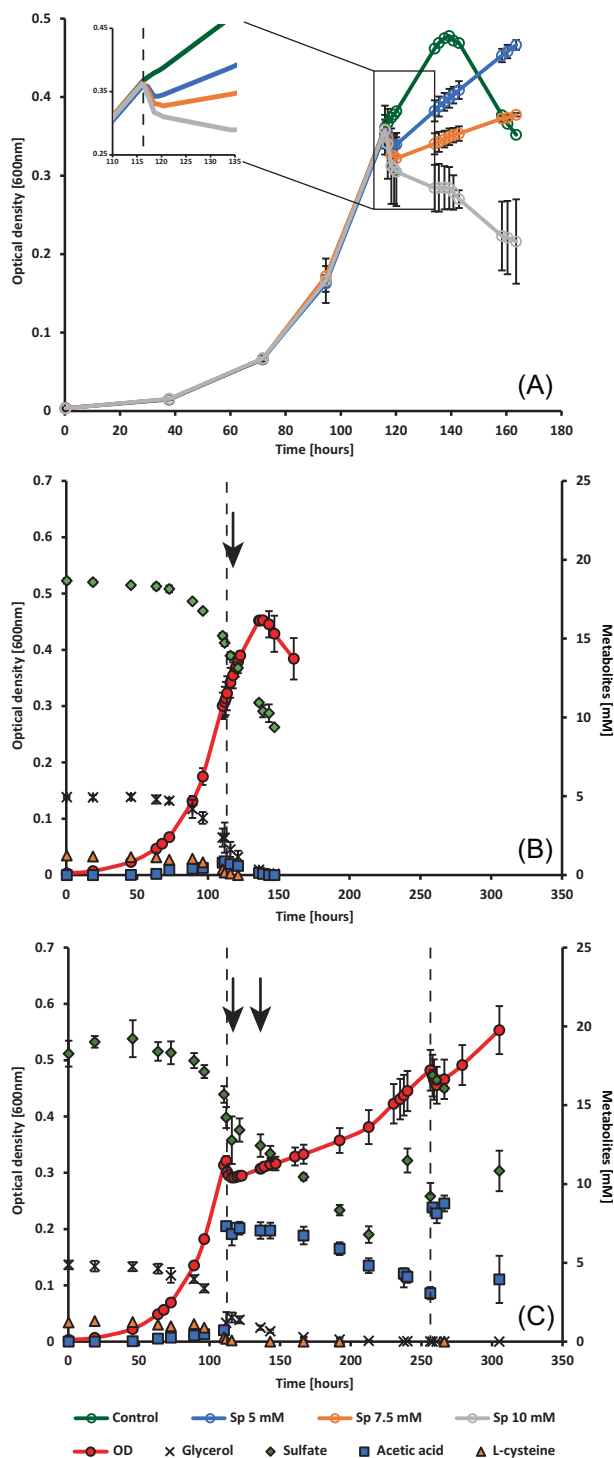
FIGURE 1 Optical density (600 nm) and concentrations of glycerol, sulfate, acetic acid, and L-cysteine in *Acididesulfobacillus acetoxydans* cultures grown for control and stressed conditions. Bioreactors were run in triplicate and pH was controlled at pH 5.0. The error bars indicate standard deviations. The black dashed lines indicate where the cultures were either spiked with water (B) or 7.5 mM acetic acid (C). The black arrows indicate the time points when samples for transcriptomics were taken. In (C) the cultures were supplemented with 5 mM sulfate after 240 h and 261 h. A second dashed line indicates a second spike with 5 mM of acetic acid until 8.5 mM of acetic acid after 261 h.

clearly shows the higher energy expenditure of *A. acetoxydans*, particularly the raise thereof with increasing acetic acid concentrations. To investigate the fast response mechanisms to acetic acid toxicity, 7.5 mM acetic acid was selected as spiking concentration as this was the maximum sub-lethal concentration for *A. acetoxydans*.

The control and test cultivations were highly similar in growth rate and metabolic activity (Figure 1B, C). In the control, no abrupt change in OD_{600} or metabolic profile was observed ultimately reaching a maximum averaged OD_{600} of 0.45 (Figure 1B). In the stressed condition, after spiking until 7.5 mM acetic acid, a decline of approximately 9% in the OD_{600} was observed, which lasted 4 h (Figure 1C). After this, *A. acetoxydans* cells resumed growth at a reduced growth rate with a doubling time of 220.6 h^{-1}. After the spike, both glycerol and acetate oxidation halted only to resume concurrent with resumed increase in OD_{600}. In the control condition glycerol was incompletely oxidized, and acetate accumulated intermittently. Concurrent consumption of acetate and glycerol started when glycerol concentration reached approximately 1.5 mM (110 h). Conversely, in the acetic-acid spike condition, acetate oxidation only started upon nearing glycerol depletion at 167 h. After the depletion of glycerol, *A. acetoxydans* continued using acetic acid as carbon source and electron donor. After prolonged acetic acid exposure, the addition of an additional 5 mM acetic acid later in the cultivation still showed a stagnation in the growth curve. This indicates that despite complete acetate oxidation and prolonged exposure, acetic acid in similar concentrations likely still affects metabolic activity of *A. acetoxydans*.

Acetic acid spike impacts gene expression profiles

Samples for gene expression analysis were taken from all the reactors 2.5 h after spiking Ac-Sp1 (Figure 1B, C). One more sample, Ac-Sp2, was taken 26 h after the second acetic acid spike in the acetic acid-spiked reactors. Control reactors were also sampled at 2.5 h after spike with water.

Of the 4104 annotated *A. acetoxydans* genes, a total of 861 genes were considered not expressed (<10 TPM in all conditions). An overview of the genes, their annotation and expression levels can be found in Supplementary File 1. Pairwise comparisons for the three conditions (control, Ac-Sp1 and Ac-Sp2) showed that the highest amount of differentially expressed genes (DEGs) were observed when comparing Ac-Sp1 to either the control (386), or Ac-Sp2 (245) (Supplementary File 1). When comparing the control to Ac-Sp2 only 148 DEGs were detected, with Ac-Sp2 resembling more to the control condition than to Ac-

Sp1. This indicated a major shift in gene expression profile of Ac-Sp1 to imposed acetic acid stress, with partially recovery in Ac-Sp2. This generates two scenarios, Ac-Sp1 sampled under highly stressed conditions and Ac-Sp2 which continued growth and is stable under similar stressed conditions. The analysis of gene expression patterns by assigning the DEGs to categories of orthologous groups indicated that the DEGs cluster mainly in category S (function unknown), E (amino acid transport and metabolism) and C (energy production and conversion) (Supplementary Table 1).

Acetic acid addition has a minor effect on central carbon and energy metabolism

Pairwise comparisons showed that in the central carbon metabolism the NAD-linked glyceraldehyde-3-phosphate dehydrogenase (*gapA*, DEACI_2591; hereafter "DEACI_" will be omitted for simplicity) was 4.2-fold upregulated in Ac-Sp1 compared to Ac-Sp2. The quinone-linked glyceraldehyde-3-phosphate dehydrogenase (*glpABC*, 1301–1303) was highly expressed, yet did not differ in expression levels. At Ac-Sp2 there was still 0.9 mM of glycerol present and no increase in acetate was observed after spiking with acetic acid despite glycerol still being present. This confirms a shift towards complete glycerol oxidation. When incompletely oxidizing glycerol, acetyl-CoA is converted by phosphate acetyltransferase (*pta*, 3443) to acetyl-phosphate and to acetate by acetate kinase (*ackA*, 3414) yielding ATP. Upon complete oxidation of glycerol or acetate, the formed acetyl-CoA enters the reverse acetyl-CoA pathway ultimately resulting in CO_2. The Pta-AckA pathway can work in reverse and the flux is thermodynamically controlled by the extracellular acetate concentration (Enjalbert et al., 2017). Interestingly, a phosphate propanoyl transferase (*pduI*, 2860), was 9.2-fold upregulated in Ac-Sp1 (compared to the control) potentially acting as alternative Pta in response to perturbation in the Pta-Ack pathway (Breitkopf et al., 2016; Liu, Leal, et al., 2007). This flux perturbation could be a mechanism for growth inhibition due to ATP expenditure next to proton and anion stress (Pinhal et al., 2019). Furthermore, acetyl phosphate is an important signalling metabolite affecting for example gene expression and acetylation of enzymes (Weinert et al., 2013; Wolfe, 2010). A comparison study with knock-outs of the Pta-Ack pathway in *Escherichia coli* proposed that the change in acetyl phosphate accounted for approximately 20% of the growth rate reduction after spiking with 128 mM acetate at pH 7.4 (0.3 mM acetic acid) (Pinhal et al., 2019). It is hypothesized that this results from interference on the acetyl phosphate regulatory function.

Regarding energy metabolism, only the heterodisulfide reductase subunits B and C (*hdrBC*, 0470-0471),

were differentially expressed being respectively 13.5 and 9.2-fold upregulated in Ac-Sp1 compared to the control. These are part of the cytoplasmic QmoAB/HdrBC complex (*qmoAB*, 0456-0457) involved in electron transfer from the quinone pool for APS reduction. Their upregulation might follow the one of the adjacent universal stress protein UspA (*uspA*, 0472). In general, universal stress proteins are synthesized after exposure to stress conditions and growth arrest (Liu, Karavolos, et al., 2007; Vollmer & Bark, 2018). UspA-encoding genes were highly upregulated in *Desulfovibrio vulgaris*, while transitioning from the exponential to stationary growth phase, and in *Desulfobacterium autotrophicum*, when growing in sulfate limited chemostats (Clark et al., 2006; Marietou et al., 2022). This aligns with the acetic acid spiking causing a temporal shift in growth phase of *A. acetoxydans*, likely triggering the expression.

No pronounced known proton stress response after acetic acid spike

A decrease in cytoplasmic pH by acetic acid dissociation is considered the main factor for organic acid toxicity. Active export of protons, cytoplasmic buffering and establishing a chemiosmotic gradient are mechanisms to maintain pH homeostasis (Baker-Austin & Dopson, 2007; Krulwich et al., 2011; Trček et al., 2015; Vergara et al., 2020). ATPases can inversely function as hydrolases, actively exporting protons at the expense of ATP. *A. acetoxydans* possesses the (highly expressed) F_oF_1-ATP synthase (*atpA-atpI*, 0352–0361) and the (medium expressed) flagellum-specific ATP synthase (*fliL*, 3788) (Supplementary Table 3). Additionally, two Na^+/H^+ antiporters (*nhaC*, 0406, 2829) and a chloride channel H^+/Cl^- antiporter (*clcA*, 0494) were medium to low expressed in all conditions showing no increased proton stress response after acetic acid spiking.

Decarboxylation of amino acids is also a proton-consuming reaction that releases CO_2. Aspartate decarboxylase (*panD*, 2148), arginine decarboxylase (*pdaD*, 0577) and glutamate decarboxylase (*gadB*, 2571) were low to medium expressed in all conditions. Glutamate decarboxylase is part of the proton-consuming γ-aminobutyrate (GABA) shunt and produces GABA from glutamate (Feehily & Karatzas, 2013). However, the majority of the GABA shunt was at negligible expression levels (Supplementary Table 3). Although a glutamate/GABA transporter was upregulated in Ac-Sp1 (*yjeM*, 3847), the role of the glutamate transporter is likely unrelated to the GABA shunt and more to the acetate anion. The urea cycle is involved in pH homeostasis through urea hydrolysis which yields two ammonia molecules and a carbamate, subsequently formed ammonia yields ammonium by incorporating a proton. *A. acetoxydans*

does not encode a urease but alternatively can use a putative urea amidolyase (0170-0171) (Hausinger, 2004; Sánchez-Andrea et al., 2022). For all different conditions, the urea amidolyase was only slightly expressed; making it unlikely to play a major role. The glycine cleavage system (*gcvABHPT*, 3684-3687), which catalyses the reversible cleavage of glycine to CO_2, methylene-THF and ammonia was upregulated in Ac-Sp1 (Kikuchi et al., 2008). Potentially this could work in reverse, as acetic acid spiking leads to increased intracellular acetyl-CoA concentrations; which could direct this complex into glycine synthesis.

Another way of preventing proton stress is inverting the membrane potential so the cell is positively charged preventing positively charged anions, including protons, from entering. This chemiosmotic gradient is considered a distinguishing feature of acidophiles (Boase et al., 2022; Buetti-Dinh et al., 2016). The importance of specifically potassium for a chemiosmotic gradient has been observed in a variety of acidophiles (Buetti-Dinh et al., 2016; Suzuki et al., 1999). The K^+-transporting ATPase (*kdpABC*, 3037-3039) was slightly expressed in all conditions. Although slightly expressed, KdpABC was not detected in the proteome of *A. acetoxydans* grown at the same pH 5.0, or even lower (pH 3.9) (Sánchez-Andrea et al., 2022). The putative regulating histidine kinase (*kdpDE*, 1068-1069), potentially involved in the control of *kdpABC* was medium expressed in all conditions (Walderhaug et al., 1992). Other cation transporters such as Na^+/Ca^{2+} and Na^+/P_i were expressed yet none differentially (Supplementary Table 2). For the role of a chemiosmotic gradient it should be noted that with organic acid stress the mode of proton entry differs. Although not differentially expressed, *kdpABC* and the other cation transporters could also contribute to the relief of osmotic stress caused by acetic acid spiking (Mira et al., 2010; Wood, 2015). Whereas often acetic acid tolerance mechanisms resolve around pH homeostasis (Li et al., 2020; Trček et al., 2015), this study shows that in *A. acetoxydans* there is no pronounced proton stress response following acetic acid spiking.

Major shifts in amino acid metabolism following acetic acid spike

After acetic acid spiking, a major fraction of the DEGs were related to the amino acid metabolism (Supplementary Table 2). The negatively charged amino acids glutamate and aspartate are the main constituents of the anion pool. Therefore, lowering their intracellular pools after acetic acid spiking maintains osmotic pressure (Pinhal et al., 2019; Roe et al., 1998; Russell, 1992). Accordingly, the generation of the amidic (alkaline) amino acids glutamine and asparagine from glutamate and aspartate via glutamine synthetase

(*glnA*, 1898) and asparaginase (*ansA*, 1809), respectively, were upregulated in Ac-Sp1 compared to the control. Another glutamine synthetase (*glnA*, 1897) was expressed but not differentially. Additionally, both glutamate synthases (*gltAB*, 1340-1341, 1344) and the aspartate amino transferase (*aspC*, 2957) were downregulated in Ac-Sp1. An aspartate ammonia-lyase (*aspA*, 0064) forming fumarate and ammonia was upregulated in Ac-Sp1. This could aid in cytoplasmic buffering by producing ammonia, which would act as a proton sink while forming ammonium. The arginine deminase system, formed by carbamate kinase (*arcC*, 3809), ornithine carbamoyltransferase (*argF*, 3810) and a putative acetylornithine deacetylase (*argE*, 3811), likely misannotated as peptidase M20, was highly upregulated in Ac-Sp1. However, the arginine biosynthesis genes encoding the steps from 2-oxoglutarate to acetyl-ornithine were downregulated in both Ac-Sp1 and Ac-Sp2 (*argCJBD*, 0927-0930; putative *argA*, 3144). The arginine pathway is notably complex and connected to a wide variety of pathways, making it complex to clearly state the function in this study (Hernández et al., 2021). The synthesis of branched chain amino acids (BCAA) is downregulated in Ac-Sp1 (*thrB, hom, ilvEDBNC, leuCDB*, 2327-2336). Multiple genes encoding amino acid transporters are actively transcribed in all conditions. Interestingly, all the downregulated amino acid transporters genes (1132-1616-1619) in Ac-Sp1 are related to BCAA transport based on their annotation. Clearly, acetic acid spiking impacted BCAA synthesis. Although organic acid, proton and anion stress affecting amino acid synthesis and concentrations is a known mechanism, the specific impact of each on BCAA synthesis is not well known. A potential a shift in BCAA synthesis might function as a response to anion pool perturbations or as acetate sink in the membrane as will be discussed later.

Acetate spike causes minor effects on biomolecules repair

Acidification of the cytoplasm increases the risk of damaging DNA, RNA and proteins (Cotter & Hill, 2003; Kültz, 2005). A variety of repair systems were expressed in all conditions, yet the majority did not change in expression levels compared to the control (Supplementary Table S4). The lack of employed proton stress mechanisms is in line with the absence of abundant DEGs in repair systems. The upregulation of some mechanisms indicates that *A. acetoxydans* is coping with stress, but does not reveal major disruption or requirement for damage control based on the gene expression profiles.

Interestingly, two ferrous iron transporters, *feoA* (2629-2630) and *feoB* (2631), were highly upregulated in Ac-Sp1. These might be controlled by the highly

upregulated ferric iron uptake regulator (*fur*, 0286, 3739). Under anaerobic conditions FeoAB can import Fe^{2+} directly into the cell (Horsburgh et al., 2001). The ferric iron regulator (Fur), is involved in the interplay of acid, oxidative and metal stress in the acidophiles *Acidithiobacillus caldus* and *Helicobacter pylori* (Chen et al., 2020; Gancz et al., 2006). *Fur*-deficient mutants of *H. pylori* are more acid sensitive and in *Salmonella enterica* the role of Fur is independent of the intracellular iron content as was shown through mutating *fur* (Bijlsma et al., 2002; Hall & Foster, 1996). Upon acid exposure, *A. caldus feoAB* was upregulated whereas *fur* was downregulated. The consensus is that *fur* works as repressor of *feoAB* (Chen et al., 2020; Deng et al., 2015), whereas in this study *fur* and *feoAB* in Sp1 are simultaneously upregulated. Transcriptional studies for both *Ds. vulgaris* and *Clostridium acetobutylicum* observed upregulation of *feoAB* upon switching from exponential to stationary growth phase (Alsaker & Papoutsakis, 2005; Clark et al., 2006). Seemingly, *fur* and *feoAB* play a role in organic acid stress, and potentially growth phase transition, for *A. acetoxydans*.

The abundance of core lipids where acetyl-CoA acts as a priming precursor increases

Biomass for core lipid analysis was harvested 8 days after being spiked with 7.5 mM acetic acid and was compared to the controls as the lipid response is slower than the transcriptome. From the *A. acetoxydans* biomass a variety of hydrolysis-derived core lipids were detected (Table 2) including fatty acid methyl esters (FAMEs, derived from hydrolysis of the intact polar lipids), hydroxy FAMEs, dimethylacetals (DMAs; formed upon acid hydrolysis of plasmalogens) and mono alkyl glycerols (derived from non-plasmalogen ether lipids, also known as alkyl ethers). The complete overview can be found in Supplementary Table S6.

The core lipid profile was dominated by the *iso*-$C_{15:0}$ fatty acid (FA), representing 41.1% in the control. The most abundant DMA and MGE in the control was also *iso*-$C_{15:0}$. The branched chain *iso*-$C_{15:0}$ FA seems to be characteristic for aSRB as it is not observed in phylogenetically related neutrophilic SRB (Sánchez-Andrea et al., 2022). Despite acetic acid spiking and a switch to acetate oxidation after glycerol depletion, the most abundant FA, *iso*-$C_{15:0}$, remained relatively unchanged in its relative abundance (approx. 36.7%). The summed percentage of the FAs, DMAs, MGEs and hydroxy-FAs did not change between the control and acetic acid-spiked cultures. Overall, comparing the acetic acid spiked condition to the control, the sum of both straight-chain and 10-methyl lipids (including FAs, hydroxy-FAs, DMAs and MGEs) increased in percentage from 3.8% to 16.9% and 2.3% to 15.5%, respectively (Table 2). Concomitantly, the sum of *iso* and *anteiso*

FAs decreased from 84.9% to 58.0%. There was no significant change in the sum of the 10-methyl *iso* and *anteiso* FAs. Changes in fatty acid composition have been observed in relation to both acetic acid and acid stress conditions in previous studies (Lindberg et al., 2013; Sohlenkamp, 2017).

A probable explanation for the observed changes in the core lipid profile is the different priming precursors of these lipids. The initiation reaction for lipid biosynthesis is the same for straight-chain and 10-methyl straight-chain lipids (both use acetyl-CoA as the precursor). Conversely for *iso* or *anteiso* branched lipids, including the 10-methyl ones, their biosynthesis depends on the FabH proteins (branched chain amino acids as the precursor).

Based on the lipid composition, the distribution of priming precursors showed a significant change. In the control, the priming precursors were made up of 6.1% acetate (acetyl-CoA), 76.6% leucine (3-methylbutyryl-CoA), 3.0% isoleucine (2-methylbutyryl-CoA) and 13.5% valine (2-methylpropanyl-CoA). In the acetic acid spiked condition this switched to 32.4% acetate 52.7% leucine, 2.7% isoleucine and 9.8% valine; suggesting a shift to acetate, or acetyl-CoA, as priming precursor in the spiked cultures (Supplementary Table 6). The acetyl-CoA-derived lipids, which increased fivefold in the spiked condition, comprise both straight chain and 10-methyl branched lipids. Of which, in the control conditions, 37.7% are 10-methyl branched, while in the spiked conditions, this increased to 47.8%. It could be inferred, therefore, that a higher percentage of the unsaturated straight-chain lipid acids may have converted to 10-methyl branched lipids upon acetic acid exposure, possibly as an adaptation mechanism to maintain cell membrane integrity. Furthermore, at low pH (comparing pH 5.0–3.9) the same pattern in priming precursors and 10-methyl branched FAs was observed in *A. acetoxydans* (Sánchez-Andrea et al., 2022). We speculate that the increase in 10-methyl branched FAs may enhance the fluidity of the lipid bilayer in the acetic acid-exposed cells. Generally, *anteiso*-FAs promote a more fluid membrane structure than *iso*-FAs, as the methyl branch is further from the end of the fatty acid, which is beneficial at low pH (Giotis et al., 2007; Zhang & Rock, 2008). By extension, mid-branching may promote membrane fluidity to an even higher degree than *iso* or *anteiso* branching as has been suggested from molecular dynamics simulations (Poger et al., 2014).

Despite this shift in the lipids, no pronounced differences in the transcription of the lipid synthesis genes was found in Ac-Sp1 or Ac-Sp2 (Supplementary Table 5). Beta-ketoacyl-ACP synthase III (*fabH*, 3409), which is involved in the selectivity for the *iso* or *anteiso* branched chain lipids, was expressed in all conditions. The *iso* or *anteiso* branched chain amino acid transaminase (*ilvE*, 2329) can transaminate leucine for the production of *iso*-odd number carbon chain fatty acids

TABLE 2 Overview of the relative abundance (% of total) of fatty acids and ether lipids including their standard deviations of A. acetoxydans in both the control (duplicate), and acetic acid spiked conditions (triplicate). Lipids that compose > 3% of total per condition are indicated in this table, the complete table can be found in Supplementary Table 6. For each of the categories the sum of branched lipids and unsaturated lipids is depicted where present. Here lipids are depicted as Cx: y with X being the number of carbons and y the number of double bonds, i: iso and Me: methyl group.

Lipids		Control Average	St. dev	Spiked Average	St. dev	Precursor
Fatty acids (FAMEs)	*i.* C15:0	41.1	2.7	36.7	1.0	leucine
	i. C16:0	3.1	0.4	2.2	0.3	valine
	C16:0	0.9	0.1	3.7	0.5	acetate
	10-Me C16:0	1.3	0.1	5.2	0.1	acetate
	i. C17:0	3.4	0.9	0.5	0.1	leucine
	10-Me *i.* C17:0	3.4	0.6	1.7	0.0	leucine
	Sum	61.4		62.1		
Dimethyl acetals derived from: plasmalogens (vinyl) ethers	*i.* C15:0 DMA	5.5	1.5	2.4	0.1	leucine
	i. C16:0 DMA	3.8	0.2	2.0	0.1	valine
	C16:0 DMA	1.1	0.1	5.9	0.5	acetate
	i. C17:0 DMA	5.1	1.2	1.4	0.1	leucine
	Sum	19.5		17.1		
Hydroxy-fatty acids (hydroxy FAMEs)	Sum	1.8		1.8		
Monoalkyl glycerol ethers derived from: alkyl (saturated) ethers	*i.* C15:0 1-MGE	4.1	0.8	3.0	0.3	leucine
	10-Me C16:0 1-MGE	0.7	0.1	6.6	0.3	acetate
	sum	16.8		18.7		
Total all core lipids	Sum straight-chain	3.8		16.9		
	Sum *iso* & *anteiso*	84.9		58.0		
	Sum 10-methyl straight-chain	2.3		15.5		
	Sum 10-methyl *iso* & *anteiso*	8.2		7.2		

(i.e., *iso*-C$_{15:0}$, *iso*-C$_{17:0}$). Although *ilvE* decreased in Ac-Sp1, the change was not significant. The biosynthetic steps involved in the formation of 10-methyl branched FAs in *Mycobacterium chlorophenolicum* depend on the expression of two genes, *bfaA* and *bfaB*. These are arranged as an operon, and encode for a flavin adenine dinucleotide binding reductase and a S-adenosyl-L-methionine-dependent methyltransferase, respectively (Blitzblau et al., 2021). The genome of *A. acetoxydans* encodes a methyltransferase protein homologue to the BfaB enzyme (2200), which was differentially expressed in both Ac-Sp1 and Ac-Sp2 compared to the control. However, the BfaA oxidoreductase protein performing the reduction reaction required for the conversion to the methyl branched FA was not detected in the genome. It is possible that in *A. acetoxydans*, this step might be encoded by a different oxidoreductase that is not related to BfaA.

Membrane lipids with plasmalogens (alkenyl, also known as, vinyl) ether bonds were detected in both the control and spiked conditions, comprising 19.5% and 17.1% of the total, respectively. Anaerobic plasmalogen synthesis is still poorly understood even though it is documented in a wide variety of anaerobic bacteria and

their apparent importance for membrane permeability (Goldfine, 2010, 2017). Recently, a two-gene operon consisting of *plsA* and *plsR* described in *Clostridium perfringens* or the single *plsA* gene in *Enterococcus faecalis*, were shown to encode for the proteins involved in the reductive conversion of an ester to a vinyl ether plasmalogen (Jackson et al., 2021). In addition, a close homologue to the PlsA protein (Ger) from *E. faecalis*, with variations at the N-terminal in the functional domain, has been demonstrated to produce glycerol alkyl ether lipids in some bacterial groups under anoxic conditions (Sahonero-Canavesi et al., 2022). *A. acetoxydans* encodes two potential homologues to PlsA, with a similar functional architectural domain to the *E. faecalis* PlsA protein, both were moderately expressed in all conditions (0950, 2070). Although able to produce alkyl glycerol ether lipids, we have not detected any Ger-encoding gene with a similar architecture as those producing alkyl glycerol ether lipids under anaerobic conditions (Sahonero-Canavesi et al., 2022). Putative homologues of *elbD* or *agpS* were detected, both are normally involved in the formation of glycerol ether lipids under aerobic conditions (Lorenzen et al., 2014). *A. acetoxydans* has previously

found to contain glycerophospholipids which contain both an ester linked and an ether linked acyl (fatty acid) chain. These were detected both as plasmalogens and as alkyl ethers. At low pH (comparing pH 5.0–3.9), the fraction of alkyl ether-bound lipids increased, potentially being a protection mechanism against acid stress (Sánchez-Andrea et al., 2022). However, no changes in the relative abundance of ether-bound lipids were found in the current study on acetic acid stress.

Ecological significance

The capability of *A. acetoxydans* to tolerate and detoxify acetic acid coupled to the reduction of sulfate underlines the ability of aSRB to ameliorate AMD. Metabolic activity of aSRB can create milder niches where less acidophilic microorganisms can thrive, facilitating the higher microbial diversity and biogeochemical cycles found in the sediment of AMD compared to the water column (Méndez-García et al., 2015; Sánchez-Andrea et al., 2011). The contribution of biosulfidogenesis on AMD attenuation is tightly linked, but is limited by carbon availability (Ayala-Muñoz et al., 2022; Sánchez-España et al., 2020; van der Graaf et al., 2020). To date, there is no in-situ data of aSRB and their contribution to biosulfidogenesis across AMD. Recently, an exhaustive study on the effect of glycerol amendment on AMD using incubation columns was performed with sediment from different AMD-impacted sites (Ilin et al., 2022). Glycerol amendment strongly triggered biosulfidogenesis, leading to an increased pH and near complete removal of soluble metals (Ilin et al., 2022). Microbial community analysis showed that in glycerol amended columns *A. acetoxydans* was among the dominant community members, where it was hypothesized to remove the accumulated acetic acid (Ilin et al., 2022).

This study showed the inhibitory effect of acetic acid spiking on the metabolic activity of *A. acetoxydans*. This has implications for the utilization of non-homogeneous, or more complex, substrates such as domestic wastewater for either in-situ bioremediation or biosulfidogenic processes (Ayala-Muñoz et al., 2022; Ñancucheo et al., 2017; Sánchez-Andrea et al., 2012; Santos & Johnson, 2022). Even without organic acid supplementation, from more complex substrates, flanking communities (e.g., fermenting microorganisms) could increase the organic acid concentrations and disrupt these processes. Furthermore, the disruptive effect of the acetate anion indicates that organic toxicity might affect microorganisms that otherwise could withstand the environmental stressors. Next to acetic acid toxicity, this study shows that the substrate composition also affects membrane composition. However, to what extent and the effect thereof on tolerating others stress factors such as pH, hydrogen sulfide and heavy metals are not known. Further research is needed on how shifting electron donor to fuel biosulfidogenesis could affect the susceptibility and composition of the sulfidogenic microbial community to endure and treat AMD.

CONCLUDING REMARKS

Acetic acid spikes of 5.0 and 7.5 hampered the growth of the aSRB *A. acetoxydans*, and a spike of 10.0 mM acetic acid resulted in complete growth inhibition. In the
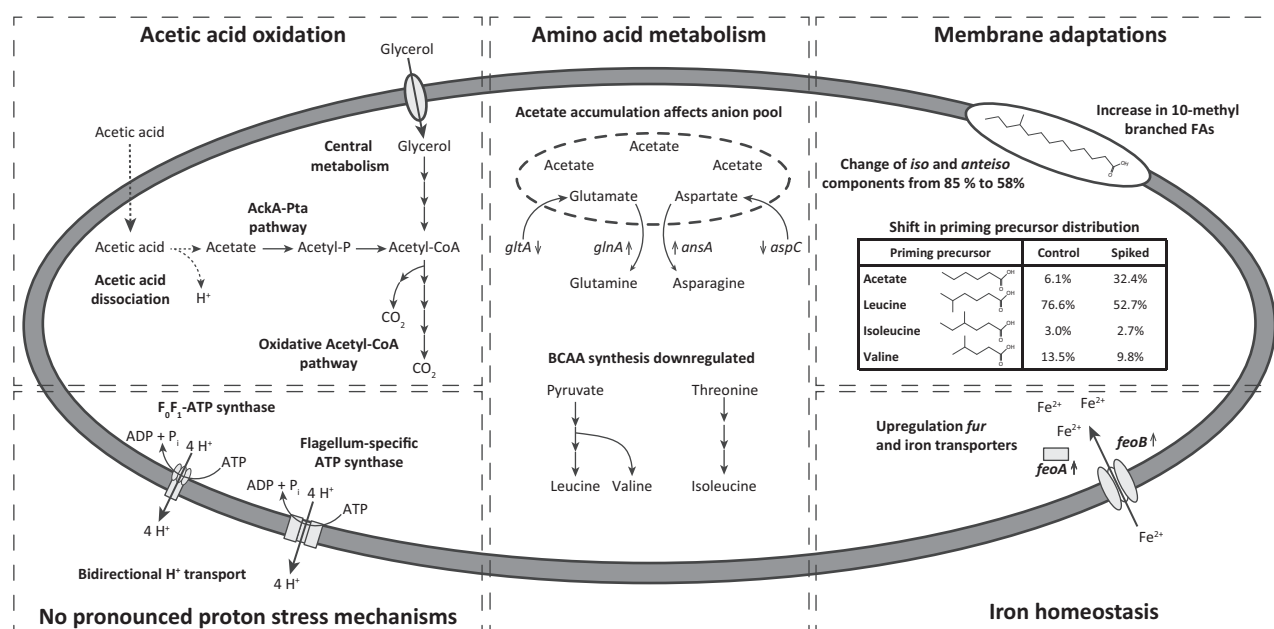

FIGURE 2   Identified acetic acid-related response mechanisms of *Acididesulfobacillus acetoxydans*.

presence of 5.0 and 7.5 mM acetic acid growth occurred at increased energy expenditure, than in control conditions (no acetic acid spike). Acetic acid toxicity is often related to cytoplasmic acidification. Gene expression profiles of *A. acetoxydans* indicate that anion accumulation is likely the main stressor, specifically the changed expression levels of genes involved in the biosynthesis and utilization of negatively charged amino acids during acetic acid spikes. Seemingly, this internal anion shift also caused a shift towards complete oxidation of glycerol. Prolonged exposure to acetic acid results in a changed membrane composition, which is accompanied by a shift in fatty acid priming precursors towards acetyl-CoA. We hypothesize that an activation of the lipid fatty acids biosynthetic pathway can reduce stress conditions by functioning as acetate sink. To compensate for the decreased membrane fluidity, caused by a decrease in branched priming precursors, there is an increase in particularly of 10-methyl branched FA. An overview of identified mechanisms in this study is depicted in Figure 2. Insights in the stress physiology and metabolic capabilities of aSRB would increase the understanding of both their ecological role and potential for bioremediation.

AUTHOR CONTRIBUTIONS

ACKNOWLEDGEMENTS

CONFLICT OF INTEREST STATEMENT

The authors declare no conflicts of interest.

DATA AVAILABILITY STATEMENT

The datasets for this study are deposited in online repositories. The transcriptome raw reads can be found at https://www.ebi.ac.uk/ena/browser/view/PRJEB64580. The genome for *Acididesulfobacillus acetoxydans* is publicly available and can be found at https://www.ebi.ac.uk/ena/browser/view/PRJEB7665 (Sánchez-Andrea et al., 2022).

ORCID

Reinier A. Egas https://orcid.org/0000-0003-1823-2179

REFERENCES

Alazard, D., Joseph, M., Battaglia-Brunet, F., Cayol, J.L. & Ollivier, B. (2010) *Desulfosporosinus acidiphilus* sp. nov.: a moderately acidophilic sulfate-reducing bacterium isolated from acid mining drainage sediments. *Extremophiles*, 14, 305–312.

Alexander, B., Leach, S. & Ingledew, W.J. (1987) The relationship between chemiosmotic parameters and sensitivity to anions and organic acids in the acidophile *Thiobacillus ferrooxidans*. *Journal of General Microbiology*, 133, 1171–1179.

Alsaker, K.V. & Papoutsakis, E.T. (2005) Transcriptional program of early sporulation and stationary-phase events in *Clostridium acetobutylicum*. *Journal of Bacteriology*, 187, 7103–7118.

Andrews, S., Krueger, F., Seconds-Pichon, A., Biggins, F. & Wingett, S. (2015) FastQC. A quality control tool for high throughput sequence data. The Babraham Institute (pp. 1). http://www.bioinformatics.bbsrc.ac.uk/projects/fastqc/.

Ayala-Muñoz, D., Burgos, W.D., Sánchez-España, J., Falagán, C., Couradeau, E. & Macalady, J.L. (2022) Novel microorganisms contribute to biosulfidogenesis in the deep layer of an acidic pit lake. *Frontiers in Bioengineering and Biotechnology*, 10, 1129.

Baker-Austin, C. & Dopson, M. (2007) Life in acid: pH homeostasis in acidophiles. *Trends in Microbiology*, 15, 165–171.

Bale, N.J., Irene Rijpstra, W.C., Sahonero-Canavesi, D.X., Oshkin, I.Y., Belova, S.E., Dedysh, S.N. et al. (2019) Fatty acid and hopanoid adaption to cold in the methanotroph *Methylovulum psychrotolerans*. *Frontiers in Microbiology*, 10, 589.

Bijlsma, J.J.E., Waidner, B., Van Vliet, A.H.M., Hughes, N.J., Häg, S., Bereswill, S. et al. (2002) The helicobacter pylori homologue of the ferric uptake regulator is involved in acid resistance. *Infection and Immunity*, 70, 606–611.

Blitzblau, H.G., Consiglio, A.L., Teixeira, P., Crabtree, D.V., Chen, S., Konzock, O. et al. (2021) Production of 10-methyl branched fatty acids in yeast. *Biotechnology for Biofuels*, 14, 1–17.

Boase, K., González, C., Vergara, E., Neira, G., Holmes, D. & Watkin, E. (2022) Prediction and inferred evolution of acid tolerance genes in the biotechnologically important Acidihalobacter genus. *Frontiers in Microbiology*, 13, 914.

Bolger, A.M., Lohse, M. & Usadel, B. (2014) Trimmomatic: a flexible trimmer for Illumina sequence data. *Bioinformatics*, 30, 2114–2120.

Breitkopf, R., Uhlig, R., Drenckhan, T. & Fischer, R.J. (2016) Two propanediol utilization-like proteins of *Moorella thermoacetica* with phosphotransacetylase activity. *Extremophiles*, 20, 653–661.

Buetti-Dinh, A., Dethlefsen, O., Friedman, R. & Dopson, M. (2016) Transcriptomic analysis reveals how a lack of potassium ions increases *Sulfolobus acidocaldarius* sensitivity to pH changes. *Microbiol (United Kingdom)*, 162, 1422–1434.

Chen, X.k., Li, X.Y., Ha, Y.F., Lin, J.Q., Liu, X.M., Pang, X. et al. (2020) Ferric uptake regulator provides a new strategy for acidophile adaptation to acidic ecosystems. *Applied and Environmental Microbiology*, 86, e00268-20.

Clark, M.E., He, Q., He, Z., Huang, K.H., Alm, E.J., Wan, X.F. et al. (2006) Temporal transcriptomic analysis as *Desulfovibrio vulgaris* Hildenborough transitions into stationary phase during electron donor depletion. *Applied and Environmental Microbiology*, 72, 5578–5588.

Cotter, P.D. & Hill, C. (2003) Surviving the acid test: responses of gram-positive bacteria to low pH. *Microbiology and Molecular Biology Reviews*, 67, 429–453.

Deng, Z., Wang, Q., Liu, Z., Zhang, M., Machado, A.C.D., Chiu, T.P. et al. (2015) Mechanistic insights into metal ion activation and operator recognition by the ferric uptake regulator. *Nature Communications*, 6, 1–12.

Enjalbert, B., Millard, P., Dinclaux, M., Portais, J.C. & Létisse, F. (2017) Acetate fluxes in *Escherichia coli* are determined by the thermodynamic control of the Pta-AckA pathway. *Scientific Reports*, 7, 1–11.

Ewels, P., Magnusson, M., Lundin, S. & Käller, M. (2016) MultiQC: summarize analysis results for multiple tools and samples in a single report. *Bioinformatics*, 32, 3047–3048.

Feehily, C. & Karatzas, K.A.G. (2013) Role of glutamate metabolism in bacterial responses towards acid and other stresses. *Journal of Applied Microbiology*, 114, 11–24.

Frolov, E.N., Kublanov, I.V., Toshchakov, S.V., Samarov, N.I., Novikov, A.A., Lebedinsky, A.V. et al. (2017) *Thermodesulfobium acidiphilum* sp. nov., a thermoacidophilic, sulfate-reducing, chemoautotrophic bacterium from a thermal site. *International Journal of Systematic and Evolutionary Microbiology*, 67, 1482–1485.

Gancz, H., Censini, S. & Merrell, D.S. (2006) Iron and pH homeostasis intersect at the level of fur regulation in the gastric pathogen *Helicobacter pylori*. *Infection and Immunity*, 74, 602–614.

Giotis, E.S., McDowell, D.A., Blair, I.S. & Wilkinson, B.J. (2007) Role of branched-chain fatty acids in pH stress tolerance in listeria monocytogenes. *Applied and Environmental Microbiology*, 73, 997–1001.

Goldfine, H. (2010) The appearance, disappearance and reappearance of plasmalogens in evolution. *Progress in Lipid Research*, 49, 493–498.

Goldfine, H. (2017) The anaerobic biosynthesis of plasmalogens. *FEBS Letters*, 591, 2714–2719.

Grime, J.M.A., Edwards, M.A., Rudd, N.C. & Unwin, P.R. (2008) Quantitative visualization of passive transport across bilayer lipid membranes. *Proceedings of the National Academy of Sciences of the United States of America*, 105, 14277–14282.

Hall, H.K. & Foster, J.W. (1996) The role of fur in the acid tolerance response of salmonella typhimurium is physiologically and genetically separable from its role in iron acquisition. *Journal of Bacteriology*, 178, 5683–5691.

Hallberg, K.B. (2010) New perspectives in acid mine drainage microbiology. In: *Hydrometallurgy*, Vol. 104. Amsterdam, The Netherlands: Elsevier, pp. 448–453.

Hausinger, R.P. (2004) Metabolic versatility of prokaryotes for urea decomposition. *Journal of Bacteriology*, 186, 2520–2522.

Hedrich, S. & Schippers, A. (2020) Distribution of acidophilic microorganisms in natural and man-made acidic environments. *Current Issues in Molecular Biology*, 40, 25–48.

Hernández, V.M., Arteaga, A. & Dunn, M.F. (2021) Diversity, properties and functions of bacterial arginases. *FEMS Microbiology Reviews*, 45, 1–26.

Herrero, A.A., Gomez, R.F., Snedecor, B., Tolman, C.J. & Roberts, M.F. (1985) Growth inhibition of clostridium thermocellum by carboxylic acids: a mechanism based on uncoupling by weak acids. *Applied Microbiology and Biotechnology*, 22, 53–62.

Horsburgh, M.J., Ingham, E. & Foster, S.J. (2001) In Staphylococcus aureus, fur is an interactive regulator with PerR, contributes to virulence, and is necessary for oxidative stress resistance through positive regulation of catalase and iron homeostasis. *Journal of Bacteriology*, 183, 468–475.

Huerta-Cepas, J., Szklarczyk, D., Heller, D., Hernández-Plaza, A., Forslund, S.K., Cook, H. et al. (2019) EggNOG 5.0: a hierarchical, functionally and phylogenetically annotated orthology resource based on 5090 organisms and 2502 viruses. *Nucleic Acids Research*, 47, D309–D314.

Ilin, A.M., van der Graaf, C.M., Yusta, I., Sorrentino, A., Sánchez-Andrea, I. & Sánchez-España, J. (2022) Glycerol amendment enhances biosulfidogenesis in acid mine drainage-affected areas: an incubation column experiment. *Frontiers in Bioengineering and Biotechnology*, 10, 978728.

Jackson, D.R., Cassilly, C.D., Plichta, D.R., Vlamakis, H., Liu, H., Melville, S.B. et al. (2021) Plasmalogen biosynthesis by anaerobic bacteria: identification of a two-gene operon responsible for plasmalogen production in *Clostridium perfringens*. *ACS Chemical Biology*, 16, 6–13.

Johnson, D.B. & Hallberg, K.B. (2005) Acid mine drainage remediation options: a review. *Science of The Total Environment*, 338, 3–14.

Johnson, D.B. & Sánchez-Andrea, I. (2019) Dissimilatory reduction of sulfate and zero-valent sulfur at low pH and its significance for bioremediation and metal recovery. *Advances in Microbial Physiology*, 75, 205–231.

Johnson, D.B. & Santos, A.L. (2020) Biological removal of sulfurous compounds and metals from inorganic wastewaters. In: *Environmental Technologies to Treat Sulfur Pollution*, pp. 215–246. London, UK: IWA Publishing.

Kaksonen, A.H., Plumb, J.J., Franzmann, P.D. & Puhakka, J.A. (2004) Simple organic electron donors support diverse sulfate-reducing communities in fluidized-bed reactors treating acidic metal- and sulfate-containing wastewater. *FEMS Microbiology Ecology*, 47, 279–289.

Kefeni, K.K., Msagati, T.A.M. & Mamba, B.B. (2017) Acid mine drainage: prevention, treatment options, and resource recovery: a review. *Journal of Cleaner Production*, 151, 475–493.

Kikuchi, G., Motokawa, Y., Yoshida, T. & Hiraga, K. (2008) Glycine cleavage system: reaction mechanism, physiological significance, and hyperglycinemia. *Proceedings of the Japan Academy. Series B, Physical and Biological Sciences*, 84, 246–263.

Krulwich, T.A., Sachs, G. & Padan, E. (2011) Molecular aspects of bacterial pH sensing and homeostasis. *Nature Reviews. Microbiology*, 9, 330–343.

Kültz, D. (2005) Molecular and evolutionary basis of the cellular stress response. *Annual Review of Physiology*, 67, 225–257.

Li, H. & Durbin, R. (2010) Fast and accurate long-read alignment with burrows-wheeler transform. *Bioinformatics*, 26, 589–595.

Li, H., Handsaker, B., Wysoker, A., Fennell, T., Ruan, J., Homer, N. et al. (2009) The sequence alignment/map format and SAMtools. *Bioinformatics*, 25, 2078–2079.

Li, Y., Wu, Z., Li, R., Miao, Y., Weng, P. & Wang, L. (2020) Integrated transcriptomic and proteomic analysis of the acetic acid stress in Issatchenkia orientalis. *Journal of Food Biochemistry*, 44, 13203.

Liao, Y., Smyth, G.K. & Shi, W. (2014) FeatureCounts: an efficient general purpose program for assigning sequence reads to genomic features. *Bioinformatics*, 30, 923–930.

Lindberg, L., Santos, A.X.S., Riezman, H., Olsson, L. & Bettiga, M. (2013) Lipidomic profiling of *Saccharomyces cerevisiae* and *Zygosaccharomyces bailii* reveals critical changes in lipid composition in response to acetic acid stress. *PLoS One*, 8, e73936.

Liu, W.T., Karavolos, M.H., Bulmer, D.M., Allaoui, A., Hormaeche, R. D.C.E., Lee, J.J. et al. (2007) Role of the universal stress protein UspA of salmonella in growth arrest, stress and virulence. *Microbial Pathogenesis*, 42, 2–10.

Liu, Y., Leal, N.A., Sampson, E.M., Johnson, C.L.V., Havemann, G.D. & Bobik, T.A. (2007) PduL is an evolutionarily distinct phosphotransacylase involved in B 12-dependent 1,2-propanediol degradation by salmonella enterica serovar typhimurium LT2. *Journal of Bacteriology*, 189, 1589–1596.

Lorenzen, W., Ahrendt, T., Bozhüyük, K.A.J. & Bode, H.B. (2014) A multifunctional enzyme is involved in bacterial ether lipid biosynthesis. *Nature Chemical Biology*, 10, 425–427.

Love, M.I., Huber, W. & Anders, S. (2014) Moderated estimation of fold change and dispersion for RNA-seq data with DESeq2. *Genome Biology*, 15, 1–21.

Marietou, A., Kjeldsen, K.U., Glombitza, C. & Jørgensen, B.B. (2022) Response to substrate limitation by a marine sulfate-reducing bacterium. *The ISME Journal*, 16, 200–210.

Méndez-García, C., Peláez, A.I., Mesa, V., Sánchez, J., Golyshina, O.V. & Ferrer, M. (2015) Microbial diversity and metabolic networks in acid mine drainage habitats. *Frontiers in Microbiology*, 6, 475.

Mira, N.P., Palma, M., Guerreiro, J.F. & Sá-Correia, I. (2010) Genome-wide identification of *Saccharomyces cerevisiae* genes required for tolerance to acetic acid. *Microbial Cell Factories*, 9, 1–13.

Mori, K., Kim, H., Kakegawa, T. & Hanada, S. (2003) A novel lineage of sulfate-reducing microorganisms: Thermodesulfobiaceae fam. Nov., *Thermodesulfobium narugense*, gen. Nov., sp. nov., a new thermophilic isolate from a hot spring. *Extremophiles*, 7, 283–290.

Ñancucheo, I. & Barrie Johnson, D. (2014) Removal of sulfate from extremely acidic mine waters using low pH sulfidogenic bioreactors. *Hydrometallurgy*, 150, 222–226.

Ñancucheo, I., Bitencourt, J.A.P., Sahoo, P.K., Alves, J.O., Siqueira, J.O. & Oliveira, G. (2017) Recent developments for remediating acidic mine waters using sulfidogenic bacteria. *BioMed Research International*, 2017, 2017.

Ñancucheo, I. & Johnson, D.B. (2012) Selective removal of transition metals from acidic mine waters by novel consortia of acidophilic sulfidogenic bacteria. *Microbial Biotechnology*, 5, 34–44.

Panova, I.A., Ikkert, O., Avakyan, M.R., Kopitsyn, D.S., Mardanov, A.V., Pimenov, N.V. et al. (2021) Desulfosporosinus metallidurans sp. nov., an acidophilic, metal-resistant sulfate-reducing bacterium from acid mine drainage. *International Journal of Systematic and Evolutionary Microbiology*, 71, 004876.

Parbhakar-Fox, A. & Lottermoser, B.G. (2015) A critical review of acid rock drainage prediction methods and practices. *Minerals Engineering*, 82, 107–124.

Park, I., Tabelin, C.B., Jeon, S., Li, X., Seno, K., Ito, M. et al. (2019) A review of recent strategies for acid mine drainage prevention and mine tailings recycling. *Chemosphere*, 219, 588–606.

Peiffer, S. (2016) Reaction time scales for sulphate reduction in sediments of acidic pit lakes and its relation to in-lake acidity neutralisation. *Applied Geochemistry*, 73, 8–12.

Pinhal, S., Ropers, D., Geiselmann, J. & De Jong, H. (2019) Acetate metabolism and the inhibition of bacterial growth by acetate. *Journal of Bacteriology*, 201, e00147-00119.

Poger, D., Caron, B. & Mark, A.E. (2014) Effect of methyl-branched fatty acids on the structure of lipid bilayers. *The Journal of Physical Chemistry B*, 118, 13838–13848.

Roe, A.J., McLaggan, D., Davidson, I., O'Byrne, C. & Booth, I.R. (1998) Perturbation of anion balance during inhibition of growth of *Escherichia coli* by weak acids. *Journal of Bacteriology*, 180, 767–772.

Russell, J.B. (1992) Another explanation for the toxicity of fermentation acids at low pH: anion accumulation versus uncoupling. *The Journal of Applied Bacteriology*, 73, 363–370.

Sahonero-Canavesi, D.X., Siliakus, M.F., Asbun, A.A., Koenen, M., von Meijenfeldt, F.A.B., Boeren, S. et al. (2022) Disentangling the lipid divide: identification of key enzymes for the biosynthesis of membrane-spanning and ether lipids in bacteria. *Science Advances*, 8, 487849.

Sánchez-Andrea, I., Rodríguez, N., Amils, R. & Sanz, J.L. (2011) Microbial diversity in anaerobic sediments at Río Tinto, a naturally acidic environment with a high heavy metal content. *Applied and Environmental Microbiology*, 77, 6085–6093.

Sánchez-Andrea, I., Sanz, J.L., Bijmans, M.F.M. & Stams, A.J.M. (2014) Sulfate reduction at low pH to remediate acid mine drainage. *Journal of Hazardous Materials*, 269, 98–109.

Sánchez-Andrea, I., Stams, A.J.M., Amils, R. & Sanz, J.L. (2013) Enrichment and isolation of acidophilic sulfate-reducing bacteria from Tinto River sediments. *Environmental Microbiology Reports*, 5, 672–678.

Sánchez-Andrea, I., Stams, A.J.M., Hedrich, S., Ñancucheo, I. & Johnson, D.B. (2015) *Desulfosporosinus acididurans* sp. nov.: an acidophilic sulfate-reducing bacterium isolated from acidic sediments. *Extremophiles*, 19, 39–47.

Sánchez-Andrea, I., Triana, D. & Sanz, J.L. (2012) Bioremediation of acid mine drainage coupled with domestic wastewater treatment. *Water Science and Technology*, 66, 2425–2431.

Sánchez-Andrea, I., van der Graaf, C.M., Hornung, B., Bale, N.J., Jarzembowska, M., Sousa, D.Z. et al. (2022) Acetate degradation at low pH by the moderately acidophilic sulfate reducer *Acididesulfobacillus acetoxydans* gen. nov. sp. nov. *Frontiers in Microbiology*, 13, 816605.

Sánchez-España, J., Yusta, I., Ilin, A., van der Graaf, C. & Sánchez-Andrea, I. (2020) Microbial geochemistry of the acidic saline pit Lake of Brunita mine (La Unión, SE Spain). *Mine Water and the Environment*, 39, 535–555.

Santos, A.L. & Johnson, D.B. (2018) Design and application of a low pH upflow biofilm sulfidogenic bioreactor for recovering transition metals from synthetic waste water at a Brazilian copper mine. *Frontiers in Microbiology*, 9, 2051.

Santos, A.L. & Johnson, D.B. (2022) Comparison of different small molecular weight alcohols for sustaining sulfidogenic bioreactors maintained at moderately low pH. *Frontiers in Bioengineering and Biotechnology*, 10, 1348.

Slonczewski, J.L., Fujisawa, M., Dopson, M. & Krulwich, T.A. (2009) Cytoplasmic pH measurement and homeostasis in bacteria and archaea. *Advances in Microbial Physiology*, 55, 1–317.

Sohlenkamp, C. (2017) Membrane homeostasis in bacteria upon pH challenge. In: *Biogenesis of fatty acids, lipids and membranes*. Cham, Switzerland: Springer International Publishing, pp. 1–13.

Stams, A.J.M., van Dijk, J.B., Dijkema, C. & Plugge, C.M. (1993) Growth of syntrophic propionate-oxidizing bacteria with fumarate in the absence of methanogenic bacteria. *Applied and Environmental Microbiology*, 59, 1114–1119.

Suzuki, I., Lee, D., Mackay, B., Harahuc, L. & Oh, J.K. (1999) Effect of various ions, pH, and osmotic pressure on oxidation of elemental sulfur by *Thiobacillus thiooxidans*. *Applied and Environmental Microbiology*, 65, 5163–5168.

Trček, J., Mira, N.P. & Jarboe, L.R. (2015) Adaptation and tolerance of bacteria against acetic acid. *Applied Microbiology and Biotechnology*, 99, 6215–6229.

van der Graaf, C.M., Sánchez-España, J., Yusta, I., Ilin, A., Shetty, S.A., Bale, N.J. et al. (2020) Biosulfidogenesis mediates natural attenuation in acidic mine pit lakes. *Microorganisms*, 8, 1–26.

Vendrell, J. & Avilés, F.X. (1986) Complete amino acid analysis of proteins by dabsyl derivatization and reversed-phase liquid chromatogrphy. *Journal of Chromatography. A*, 358, 401–413.

Vergara, E., Neira, G., González, C., Cortez, D., Dopson, M. & Holmes, D.S. (2020) Evolution of predicted acid resistance mechanisms in the extremely acidophilic Leptospirillum genus. *Genes (Basel)*, 11, 389.

Vollmer, A.C. & Bark, S.J. (2018) Twenty-five years of investigating the universal stress protein: function, structure, and applications. *Advances in Applied Microbiology*, 102, 1–36.

Walderhaug, M.O., Polarek, J.W., Voelkner, P., Daniel, J.M., Hesse, J.E., Altendorf, K. et al. (1992) KdpD and KdpE, proteins that control expression of the kdpABC operon, are members of the two-component sensor-effector class of regulators. *Journal of Bacteriology*, 174, 2152–2159.

Weinert, B.T., Iesmantavicius, V., Wagner, S.A., Schölz, C., Gummesson, B., Beli, P. et al. (2013) Acetyl-phosphate is a critical determinant of lysine acetylation in *E. coli*. *Molecular Cell*, 51, 265–272.

Wolfe, A.J. (2010) Physiologically relevant small phosphodonors link metabolism to signal transduction. *Current Opinion in Microbiology*, 13, 204–209.

Wood, J.M. (2015) Bacterial responses to osmotic challenges. *The Journal of General Physiology*, 145, 381–388.

Xia, J.M. & Yuan, Y.J. (2009) Comparative lipidomics of four strains of *Saccharomyces cerevisiae* reveals different responses to furfural, phenol, and acetic acid. *Journal of Agricultural and Food Chemistry*, 57, 99–108.

Zhang, Y.M. & Rock, C.O. (2008) Membrane lipid homeostasis in bacteria. *Nature Reviews. Microbiology*, 63(6), 222–233.

SUPPORTING INFORMATION

Additional supporting information can be found online in the Supporting Information section at the end of this article.